



Design, synthesis, and bioevaluation of novel oxoindolin-2-one derivatives incorporating 1-benzyl-1H-1,2,3-triazole

Ta Thu Lan¹ · Duong Tien Anh¹ · Pham-The Hai¹ · Do Thi Mai Dung¹ · Le Thi Thu Huong² · Eun Jae Park³ · Hye Won Jeon³ · Jong Soon Kang⁴ · Nguyen Thi Thuan¹ · Sang-Bae Han³ · Nguyen-Hai Nam¹

Received: 19 September 2019 / Accepted: 29 November 2019
© Springer Science+Business Media, LLC, part of Springer Nature 2019

Abstract

In our search for novel bioactive molecules, three series of indolin-2-one derivatives incorporating 1-benzyl-1H-1,2,3-triazole moiety were synthesized. The compounds were initially designed as acetylcholine esterase (AChE) inhibitors based on the structural feature of donepezil, a known AChE inhibitor which is currently used clinically to treat Alzheimer's disease (AD). Two compounds **4g** and **3a** were found to be the most potent in inhibition of AChE with inhibition percentages of 51 and 50% when tested at the concentration of 100 μM . Docking assays were carried out in order to explain the structure–activity relationships of these compounds compared with Donepezil against AChE enzyme. In DPPH free radical-scavenging assay, most compounds showed only weak scavenging activity. Noteworthy, additional cytotoxic evaluation of the compounds against three human cancer cell lines (SW620, human colon cancer; PC3, prostate cancer; NCI-H23, lung cancer) revealed that five compounds, including **3c**, **3e**, **5c**, **5e**, and **5g**, exhibited strong cytotoxicity (IC_{50} values in the range of 0.65–7.17 μM). Compound **5g** was the most potent one with IC_{50} values as low as 0.65 μM , even more potent than adriamycin, a positive control. Thus, compound **5g** would be promising for further development as an anticancer agent.

Keywords Acetylcholine esterase inhibitors · Oxoindolin-2-one · Cytotoxicity · Docking simulation

Introduction

Alzheimer's disease (AD) is a progressive and neurodegenerative disease characterized by gradual loss of memory

and other cognitive impairments. It is the most common form of dementia (Huang and Mucke 2012; Kumar et al. 2015). Currently, the disease affect nearly 40 million individuals of people over 65 and accounts for ~80% of dementia patients worldwide (Kumar et al. 2015). It is known that many factors contribute to the initiation and progression of the disease, however, due to the complexity of the AD's etiology and pathogenesis, the principal causes of the disease remain unclear. To date, the disease is still one of the incurable neurological disorders. The clinical management of the disease relies mostly on the symptomatic treatment (Huang and Mucke 2012).

Recently, with the enormous efforts of scientists devoted in studying the AD's pathology, a number of critical factors causing the disease have been indicated, such as abnormal posttranslational modifications of tau protein, which result in neurofibrillary tangles; deposition of amyloid β -protein ($\text{A}\beta$) plaques; and a decrease in the level of the neurotransmitter acetylcholine (Olivero et al. 2014; Yiannopoulou and Papageorgiou 2013). Among these, the acetylcholine decrease in the brain is considered as one the most underlying factors. In fact, all drugs approved for the treatment of AD currently, including donepezil, tacrine,

Supplementary information The online version of this article (<https://doi.org/10.1007/s00044-019-02488-1>) contains supplementary material, which is available to authorized users.

- ✉ Sang-Bae Han
shan@cbnu.ac.kr
- ✉ Nguyen-Hai Nam
namnh@hup.edu.vn

- ¹ Hanoi University of Pharmacy, 13-15 Le Thanh Tong, Hanoi, Vietnam
- ² School of Medicine and Pharmacy, Hanoi National University, 144 Xuan Thuy, Hanoi, Vietnam
- ³ College of Pharmacy, Chungbuk National University, 194-31, Osongsaengmyung-1, Heungdeok, Cheongju, Chungbuk 28160, Republic of Korea
- ⁴ Bio-Evaluation Center, Korea Research Institute of Bioscience and Biotechnology, Cheongju, Chungbuk, Republic of Korea

galantamine, and rivastigmine (Fig. 1), are acetylcholine esterase inhibitors (Rodda and Carter 2012).

Acetylcholine esterase (AChE; EC 3.1.1.7) is a member of the serine hydrolase enzyme family. These enzymes catalyze the hydrolysis of a neurotransmitter acetylcholine, resulting in the breakdown of acetylcholine into choline and acetic acid. Consequently, the concentration of acetylcholine is decreased and the cholinergic neurotransmission is terminated (Massoulié et al. 1993). Thus, inhibition of acetylcholine esterase would prevent the hydrolysis of acetylcholine and subsequently elevate the cholinergic neurotransmission, resulting in clinical improvement of the disease. Due to the therapeutic importance of AChE in AD pathology, many medicinal chemists worldwide have devoted intensive efforts in developing novel AChE inhibitors. As a result, structurally diverse AChE inhibitors both naturally and synthetic, have been reported in the past decades (Singh et al. 2013). Joined in that efforts we have designed several series of donepezil analogs which incorporate oxindolin-2-one core imbedded with 1-benzyl-4*H*-1,2,3-triazole ring (Fig. 2). It is envisioned that the incorporation of the triazole moiety not only retains a nitrogen atom similar to that in donepezil but also introduces a heterocycle with more possible interactions with the enzyme binding site. This paper describes the synthesis and AChE inhibitory activity of these compounds series. Additional evaluation of the compounds in 1,1-diphenyl-2-

picrylhydrazil (DPPH) free radical-scavenging and cytotoxic assays is also presented.

Materials and methods

Chemistry

Thin layer chromatography, which was performed using Whatman® 250 µm Silica Gel GF Uniplates and visualized under UV light at 254 nm, was used to check the progress of reactions and preliminary evaluation of compounds' homogeneity. Melting points were measured using a Gallenkamp Melting Point Apparatus (LabMerchant, London, United Kingdom) and are uncorrected. Purification of compounds was carried out using crystallization methods and/or open silica gel column flash chromatography employing Merck silica gel 60 (240–400 mesh) as stationary phase. Nuclear magnetic resonance spectra (¹H and ¹³C NMR) were recorded on a Bruker 500 MHz spectrometer with dimethyl sulfoxide (DMSO)-*d*₆ as solvent unless otherwise indicated. Tetramethylsilane was used as an internal standard. Chemical shifts are reported in parts per million (ppm), downfield from tetramethylsilane. Mass spectra with different ionization modes including electron ionization, Electrospray ionization (ESI), were recorded using PE Biosystems API2000 (Perkin Elmer, Palo Alto,

Fig. 1 Structures of some AChE inhibitors

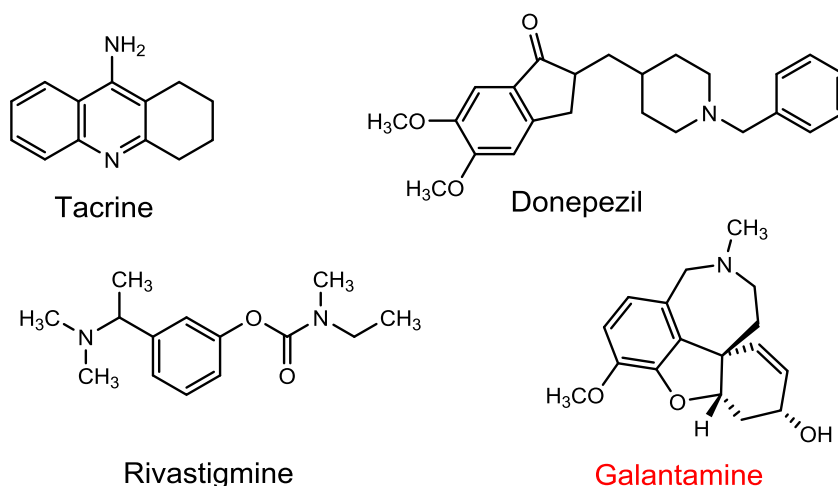
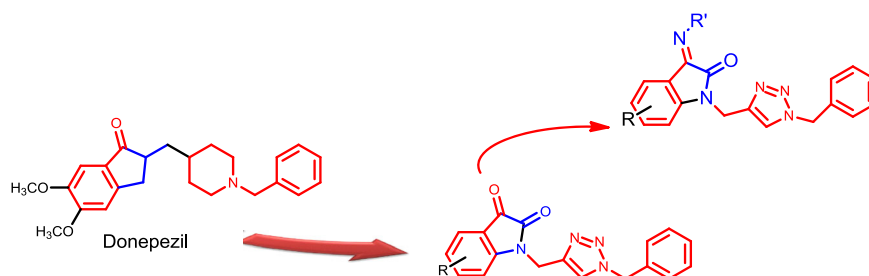


Fig. 2 Design of novel AChE inhibitors



CA, USA) and Mariner[®] (Azco Biotech, Inc. Oceanside, CA, USA) mass spectrometers, respectively. The elemental (C, H, N) analyses were performed on a Perkin Elmer model 2400 elemental analyzer. All reagents and solvents were purchased from Aldrich or Fluka Chemical Corp. (Milwaukee, WI, USA) or Merck unless noted otherwise. Solvents were used directly as purchased unless otherwise indicated.

The synthesis of novel oxoindolin-2-ones imbedded with 1-benzyl-4*H*-1,2,3-triazole scaffold (**3–5**) was carried out as illustrated in Scheme 1. Details are described below.

General procedures for the synthesis of compounds **3a–g**

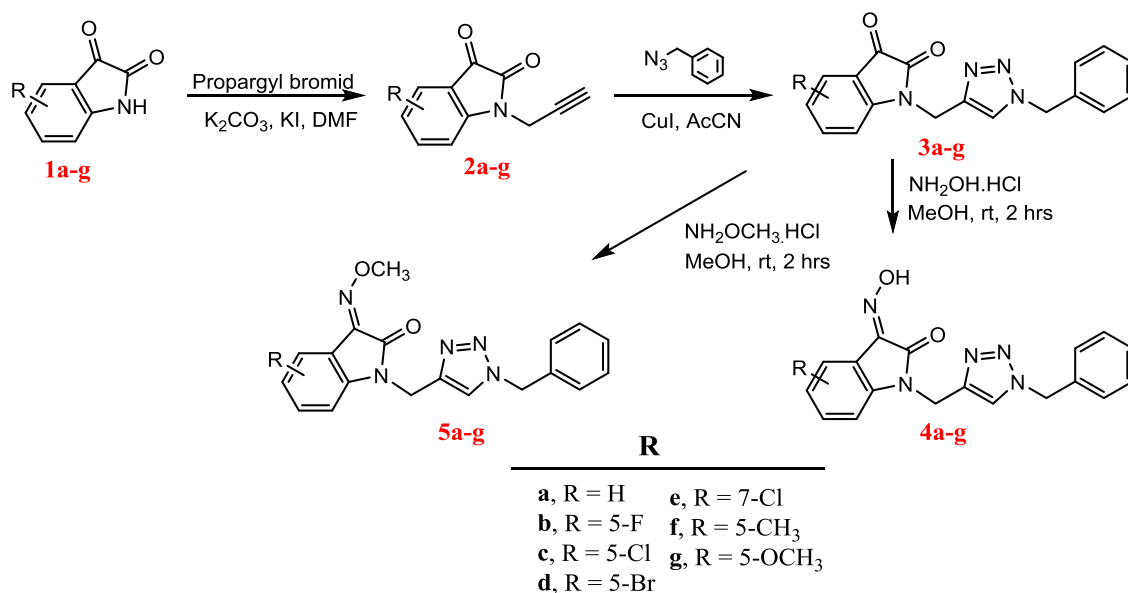
To a respective solution of isatins **1a–g** (1 mmol) in dimethylformamide (DMF) (3 mL) were added K₂CO₃ (165.5 mg, 1.2 mmol). The mixtures were stirred at 80 °C for 1 h, then then a catalytic amount of KI (8.3 mg, 0.05 mmol) was added. After stirring for further 15 min, 0.15 ml of a solution of propargyl bromide 80% in toluene was dropped slowly into the mixtures. The reaction mixtures were again stirred at 60 °C for 3 h. The reaction was checked by TLC. After the reaction completed, the resulting mixtures were cooled, poured into ice-cold water, and acidified to pH ~4. The orange solids formed were filtered and dried to give the propargylated isatins **2**, which were used for the next step without further purification.

A respective solution of compounds **2a–g** and (azido-methyl)benzene (1 mmol) in acetonitrile (10 mL) were stirred at room temperature for 10 min, then CuI (19.1 mg, 0.1 mmol) was added. The mixture was stirred at 50 °C until

the reaction completed (12–24 h). The corresponding resulting mixtures were evaporated under reduced pressure to give the residues, which were re-dissolved in 50 ml of DCM. The mixtures were filtered and the DCM layers were evaporated under reduced pressure to give the targeting compounds **3a–g**.

1-((1-Benzyl-1*H*-1,2,3-triazol-4-yl)methyl)indoline-2,3-dione (3a**)** Orange solid; Yield: 63%. mp: 173–174 °C. *R_f* = 0.65 (DCM: MeOH = 20: 1). IR (KBr, cm⁻¹): 3134 (CH, arene); 2970 (CH, CH₂); 1728 (C=O); 1611, 1468 (C=C). ¹H-NMR (500 MHz, DMSO-*d*₆, ppm): δ 8.23 (1H, s, H-6'); 7.63 (1H, t, *J* = 7.75 Hz, H-4), 7.57 (1H, d, *J* = 7.50 Hz, H-7, 7.38–7.32 (3H, m, H-4'', H-5'', H-6''), 7.27 (2H, d, *J* = 8.00 Hz, H-3'', H-7''), 7.16–7.12 (2H, m, H-5, H-6), 5.57 (2H, s, H-1''a, H-1''b), and 4.97 (2H, s, H-1'a, H-1'b). ¹³C NMR (125 MHz, DMSO-*d*₆, ppm): δ 183.51, 158.30, 150.62, 138.48, 136.35, 129.22, 128.63, 128.38, 124.91, 124.28, 123.82, 118.12, 111.62, 53.37, and 35.59. ESI-MS *m/z*: 319.20 [M + H]⁺

1-((1-Benzyl-1*H*-1,2,3-triazol-4-yl)methyl)-5-fluoroindoline-2,3-dione (3b**)** Orange solid; Yield: 67%. mp: 185–186 °C. *R_f* = 0.67 (DCM: MeOH = 20: 1). IR (KBr, cm⁻¹): 3055 (CH, arene); 2901 (CH, CH₂); 1728 (C=O); 1616, 1468 (C=C). ¹H-NMR (500 MHz, DMSO-*d*₆, ppm): 8.23 (1H, s, H-6'), 7.53–7.47 (2H, m, H-4', H-7'), 7.38–7.32 (3H, m, H-4'', H-5'', H-6''), 7.28 (2H, d, *J* = 8.00 Hz, H-3'', H-7''), 7.19–7.17 (1H, m, H₆), 5.57 (2H, s, H-1''a, H-1''b), and 4.97 (2H, s, H-1'a, H-1'b). ¹³C NMR (125 MHz, DMSO-*d*₆, ppm): δ 182.91, 159.97, 158.33, 158.05, 146.87, 142.19, 136.38, 129.22, 129.17, 128.62, 128.38, 124.48, 124.29,



Scheme 1 Synthesis of oxoindolin-2-one derivatives imbedded with 1-benzyl-4*H*-1,2,3-triazole scaffold (**3–5**)

124.26, 119.07, 119.01, 113.06, 113.00, 112.01, 111.81, 53.34, and 35.62. *ESI-MS m/z*: 337.10 [M + H]⁺

1-((1-Benzyl-1H-1,2,3-triazol-4-yl)methyl)-5-chloroindoline-2,3-dione (3c) Orange solid; Yield: 66%. mp: 191–192 °C. $R_f = 0.68$ (DCM: MeOH = 20: 1). *IR (KBr, cm⁻¹)*: 3078 (CH, arene); 2968 (CH, CH₂); 1724 (C=O); 1605, 1470 (C=C). *¹H-NMR (500 MHz, DMSO-*d*₆, ppm)*: 8.20 (1H, s, H-6'), 7.69 (1H, dd, $J = 8.50$ Hz, $J' = 2.00$ Hz, H-7), 7.63 (1H, d; $J = 2.00$ Hz, H-4), 7.38–7.32 (3H, m, H-4'', H-5'', H-6''), 7.27 (2H, d, $J = 8.00$ Hz, H-3'', H-7''), 7.15 (1H, d, $J = 8.50$ Hz, H-6), 5.57 (2H, s, H-1''a, H-1''b), and 4.97 (2H, s, H-1'a, H-1'b). *¹³C NMR (125 MHz, DMSO-*d*₆, ppm)*: δ 182.40, 158.07, 149.13, 142.09, 137.32, 136.37, 129.22, 128.63, 128.38, 128.04, 124.40, 124.23, 119.54, 113.34, 53.33, and 35.66. *ESI-MS m/z*: 353.10 [M + H]⁺

1-((1-Benzyl-1H-1,2,3-triazol-4-yl)methyl)-7-chloroindoline-2,3-dione (3d) Orange solid; Yield: 60%. mp: 193–194 °C. $R_f = 0.68$ (DCM: MeOH = 20: 1). *IR (KBr, cm⁻¹)*: 3080 (CH, arene); 2986 (CH, CH₂); 1726 (C=O); 1605, 1470 (C=C). *¹H-NMR (500 MHz, DMSO-*d*₆, ppm)*: 8.15 (1H, s, H-6'), 7.95 (1H, d, $J = 7.50$ Hz, H-4), 7.44 (1H, d, $J = 8.00$ Hz, H-6), 7.37–7.31 (3H, m, H-4'', H-5'', H-6''), 7.25 (2H, d, $J = 7.00$ Hz, H-3'', H-7''), 7.12 (1H, t, $J = 7.50$ Hz, H-5), 5.55 (2H, s, H-1''a, H-1''b), and 4.26 (2H, s, H-1'a, H-1'b). *¹³C NMR (125 MHz, DMSO-*d*₆, ppm)*: δ 163.34, 144.02, 142.46, 139.54, 136.54, 135.14, 129.18, 128.54, 128.20, 126.84, 124.84, 123.33, 118.49, 115.49, 53.26, and 37.70. *ESI-MS m/z*: 353.00 [M + H]⁺

1-((1-Benzyl-1H-1,2,3-triazol-4-yl)methyl)-5-bromoindoline-2,3-dione (3e) Orange solid; Yield: 57%. mp: 203–204 °C. $R_f = 0.65$ (DCM: MeOH = 20: 1). *IR (KBr, cm⁻¹)*: 2985 (CH, CH₂); 1728 (C=O); 1601, 1470 (C=C). *¹H-NMR (500 MHz, DMSO-*d*₆, ppm)*: 8.20 (1H, s, H-6'), 7.81 (1H, dd, $J = 8.50$ Hz, $J' = 2.00$ Hz, H-7), 7.73 (1H, d, $J = 2.00$ Hz, H-4), 7.39–7.32 (3H, m, H-4'', H-5'', H-6''), 7.28 (2H, d, $J = 7.00$ Hz, H-3'', H-7''), 7.13 (1H, d, $J = 8.00$ Hz, H-6), 5.56 (2H, s, H-1''a, H-1''b), and 4.97 (2H, s, H-1'a, H-1'b). *¹³C NMR (125 MHz, DMSO-*d*₆, ppm)*: δ 182.45, 157.91, 149.49, 140.13, 136.36, 129.22, 128.92, 128.63, 128.38, 127.13, 124.26, 119.92, 115.56, 113.77, 53.34, and 35.66. *ESI-MS m/z*: 397.00 (⁷⁹Br), 399.00 (⁸¹Br) [M + H]⁺

1-((1-Benzyl-1H-1,2,3-triazol-4-yl)methyl)-5-methylindoline-2,3-dione (3f) Orange solid; Yield: 70%. mp: 194–195 °C. $R_f = 0.67$ (DCM: MeOH = 20: 1). *IR (KBr, cm⁻¹)*: 3069 (CH, arene); 2922 (CH, CH₂); 1717 (C=O); 1597, 1487 (C=C). *¹H-NMR (500 MHz, DMSO-*d*₆, ppm)*: 8.22 (1H, s, H-6'), 7.44–7.28 (7H, m, H-4, H-7, H-4'', H-5'', H-6'', H-3'', H-7''), 7.04 (1H, d, $J = 7.5$ Hz, H₆), 5.56 (2H, s, H-1''a, H-1''b), 4.95 (2H, s, H-1'a, H-1'b), and 2.27 (3H, s, 5-CH₃).

*¹³C NMR (125 MHz, DMSO-*d*₆, ppm)*: δ 185.42, 183.76, 138.79, 136.70, 133.24, 129.33, 129.21, 128.92, 128.62, 128.58, 128.37, 125.13, 111.49, 53.68, 53.35, and 20.51. *ESI-MS m/z*: 333.20 [M + H]⁺

1-((1-Benzyl-1H-1,2,3-triazol-4-yl)methyl)-5-methoxyindoline-2,3-dione (3g) Orange solid; Yield: 55%. mp: 196–197 °C. $R_f = 0.65$ (DCM: MeOH = 20: 1). *IR (KBr, cm⁻¹)*: 3069 (CH, arene); 2901 (CH, CH₂); 1721 (C=O); 1588, 1487 (C=C). *¹H-NMR (500 MHz, DMSO-*d*₆, ppm)*: 8.20 (1H, s, H₆'), 7.36–7.34 (3H, m, H-4'', H-5'', H-6''), 7.27 (2H, d, $J = 6.50$ Hz, H-3'', H-7''), 7.24–7.21 (1H, m, H-7), 7.16 (1H, d, $J = 3.00$ Hz, H-4), 7.08 (1H, d, $J = 8.50$ Hz, H-6), 5.56 (2H, s, H-1''a, H-1''b), 4.94 (2H, s, H-1'a, H-1'b), and 3.76 (3H, s, 5-OCH₃). *¹³C NMR (125 MHz, DMSO-*d*₆, ppm)*: δ 183.80, 158.33, 156.29, 144.45, 136.39, 129.22, 128.62, 128.37, 124.29, 124.21, 118.56, 112.71, 109.68, 56.38, 53.33, and 35.54. *ESI-MS m/z*: 349.10 [M + H]⁺

General procedures for the synthesis of compounds 4

Each of the compounds **3** was dissolved in MeOH, then hydroxylamine hydrochloride (685 mg, 10 mmol) was added, followed by dropwise addition of a solution of NaOH (400 mg in 1 mL of water). The mixtures were stirred at room temperature for 2 h. At the end of this reaction, the resulting reaction mixtures were poured into ice-cold water, neutralized to pH ~ 7 and acidified by dropwise addition of a solution of HCl 5% to induce maximum precipitation. The precipitates were filtered, dried, and re-crystallised in methanol to give the targeting compounds **4**.

1-((1-Benzyl-1H-1,2,3-triazol-4-yl)methyl)-3-(hydroxyimino)indolin-2-one (4a) Yellow solid; Yield: 60%. mp: 190–191 °C. $R_f = 0.50$ (DCM: MeOH = 20: 1). *IR (KBr, cm⁻¹)*: 3119 (OH); 3007 (CH, arene); 2777 (CH, CH₂); 1717 (C=O); 1605, 1456 (C=C). *¹H-NMR (500 MHz, DMSO-*d*₆, ppm)*: 13.55 (1H, s, N-OH), 8.17 (1H, s, H-6'), 8.00 (1H, d, $J = 7.00$ Hz, H-4), 7.41–7.27 (6H, m, H-7, H-3'', H-4'', H-5'', H-6'', H-7''), 7.12–7.08 (2H, m, H-5, H-6), 5.55 (2H, s, H-1''a, H-1''b), and 4.99 (2H, s, H-1'a, H-1'b). *¹³C NMR (125 MHz, DMSO-*d*₆, ppm)*: δ 163.31, 142.96, 142.74, 136.45, 132.23, 129.20, 128.59, 128.36, 127.17, 124.02, 123.20, 110.06, 53.27, and 35.13. *ESI-MS m/z*: 334.20 [M + H]⁺

1-((1-Benzyl-1H-1,2,3-triazol-4-yl)methyl)-5-fluoro-3-(hydroxyimino)indolin-2-one (4b) Yellow solid; Yield: 56%. mp: 197–198 °C. $R_f = 0.53$ (DCM: MeOH = 20: 1). *IR (KBr, cm⁻¹)*: 3161 (OH); 3063 (CH, arene); 2814 (CH, CH₂); 1711 (C=O); 1614, 1472 (C=C). *¹H-NMR (500 MHz, DMSO-*d*₆, ppm)*: 13.78 (1H, s, N-OH), 8.17 (1H, s, H-6'),

7.77 (1H, d, $J = 7.00$ Hz, H-4), 7.38–7.27 (6H, m, H-7, H-3", H-4", H-5", H-6", H-7"), 7.15–7.10 (1H, m, H-6), 5.55 (2H, s, H-1"a, H-1"b), and 5.00 (2H, s, H-1'a, H-1'b). ^{13}C NMR (125 MHz, DMSO- d_6 , ppm): δ 136.44, 129.21, 128.60, 128.39, and 53.30. ESI-MS m/z : 352.10 [M + H] $^+$

1-((1-Benzyl-1H-1,2,3-triazol-4-yl)methyl)-5-chloro-3-(hydroxyimino)indolin-2-one (4c) Yellow solid; Yield: 55%. mp: 213–214 °C. $R_f = 0.55$ (DCM: MeOH = 20: 1). IR (KBr, cm^{-1}): 3379 (OH); 3082 (CH, arene); 2805 (CH, CH_2); 1715 (C=O); 1607, 1464 (C=C). $^1\text{H-NMR}$ (500 MHz, DMSO- d_6 , ppm): 8.18 (1H, s, H-6'), 7.94 (1H, s, H-4), 7.36–7.27 (7H, m, H-6, H-7, H-3", H-4", H-5", H-6", H-7"), 5.55 (2H, s, H-1"a, H-1"b), and 5.01 (2H, s, H-1'a, H-1'b). ^{13}C NMR (125 MHz, DMSO- d_6 , ppm): δ 142.54, 136.40, 129.21, 128.61, 128.38, 124.08, 53.31, 36.26, 35.32, and 31.25. ESI-MS m/z : 368.10 [M + H] $^+$

1-((1-Benzyl-1H-1,2,3-triazol-4-yl)methyl)-7-chloro-3-(hydroxyimino)indolin-2-one (4d) Yellow solid; Yield: 52%. mp: 219–220 °C. $R_f = 0.55$ (DCM: MeOH = 20: 1). IR (KBr, cm^{-1}): 3120 (OH); 3009 (CH, arene); 1722 (C=O); 1601, 1439 (C=C). $^1\text{H-NMR}$ (500 MHz, DMSO- d_6 , ppm): 13.87 (1H, s, N-OH), 8.14 (1H, s, H-6'), 8.08 (1H, d, $J = 7.00$ Hz, H-4), 7.51 (1H, d, $J = 8.00$ Hz, H-6), 7.42–7.28 (3H, m, H-4", H-5", H-6"), 7.25 (2H, d, $J = 7.00$ Hz, H-3", H-7"), 7.12 (1H, t, $J = 7.75$ Hz, H-5), 5.55 (2H, s, H-1"a, H-1"b), and 5.33 (2H, s, H-1'a, H-1'b). ^{13}C NMR (125 MHz, DMSO- d_6 , ppm): δ 164.13, 144.19, 142.67, 138.93, 136.57, 134.25, 129.18, 128.54, 128.19, 126.35, 124.74, 123.31, 118.81, 115.27, 53.24, and 37.57. ESI-MS m/z : 368.10 [M + H] $^+$

1-((1-Benzyl-1H-1,2,3-triazol-4-yl)methyl)-5-bromo-3-(hydroxyimino)indolin-2-one (4e) Yellow solid; Yield: 55%. mp: 228–229 °C. $R_f = 0.56$ (DCM: MeOH = 20: 1). IR (KBr, cm^{-1}): 3163 (OH); 3082 (CH, arene); 2855 (CH, CH_2); 1717 (C=O); 1603, 1466 (C=C). $^1\text{H-NMR}$ (500 MHz, DMSO- d_6 , ppm): 13.83 (1H, s, N-OH), 8.18 (1H, s, H-6'), 8.11 (1H, s, H-4), 7.62–7.13 (7H, m, H-6, H-7, H-3", H-4", H-5", H-6", H-7"), 5.55 (2H, s, H-1"a, H-1"b), and 5.00 (2H, s, H-1'a, H-1'b). ^{13}C NMR (125 MHz, DMSO- d_6 , ppm): δ 142.20, 136.40, 134.61, 129.20, 128.60, 128.37, 124.09, 112.28, 53.31, and 35.31. ESI-MS m/z : 412.10 (^{79}Br), 414.10 (^{81}Br) [M + H] $^+$

1-((1-Benzyl-1H-1,2,3-triazol-4-yl)methyl)-3-(hydroxyimino)-5-methylindolin-2-one (4f) Yellow solid; Yield: 63%. mp: 195–196 °C. $R_f = 0.54$ (DCM: MeOH = 20: 1). IR (KBr, cm^{-1}): 3123 (OH); 3082 (CH, arene); 2833 (CH, CH_2); 1717 (C=O); 1616, 1472 (C=C). $^1\text{H-NMR}$ (500 MHz, DMSO- d_6 , ppm): 13.44 (1H, s, N-OH), 8.17 (1H, s, H-6'), 8.11 (1H, s, H-4), 7.34–7.03 (7H, m, H-6, H-7, H-3", H-4", H-5", H-6", H-7"), 5.55 (2H, s, H-1"a, H-1"b), 5.00 (2H, s,

H-1'a, H-1'b), and 2.29 (3H, s, 5- CH_3). ^{13}C NMR (125 MHz, DMSO- d_6 , ppm): δ 136.43, 132.55, 129.20, 128.59, 128.36, 124.19, 110.05, 53.29, 35.27, and 20.92. ESI-MS m/z : 348.10 [M + H] $^+$

1-((1-Benzyl-1H-1,2,3-triazol-4-yl)methyl)-3-(hydroxyimino)-5-methoxyindolin-2-one (4g) Yellow solid; Yield: 53%. mp: 204–205 °C. $R_f = 0.53$ (DCM: MeOH = 20: 1). IR (KBr, cm^{-1}): 3204 (OH); 2905 (CH, CH_2); 1717 (C=O); 1614, 1481 (C=C). $^1\text{H-NMR}$ (500 MHz, DMSO- d_6 , ppm): 13.54 (1H, s, N-OH), 8.15 (1H, s, H-6'), 7.59 (1H, d, $J = 2.50$ Hz, H-4), 7.36–7.33 (7H, m, H-4", H-5", H-6"), 7.27 (2H, d, $J = 8.00$ Hz, H-3", H-7"), 7.03–7.00 (2H, m, H-6, H-7), 5.55 (2H, s, H-1"a, H-1"b), 5.00 (2H, s, H-1'a, H-1'b), and 3.73 (3H, s, 5-O CH_3). ^{13}C NMR (125 MHz, DMSO- d_6 , ppm): δ 163.10, 155.71, 144.16, 142.77, 136.70, 136.44, 129.20, 128.60, 128.36, 123.99, 117.34, 116.34, 113.58, 110.73, 56.14, 53.27, and 35.18. ESI-MS m/z : 364.10 [M + H] $^+$

General procedures for the synthesis of compounds 5

Compounds **5a–g** were synthesized via a three-step pathway as illustrated in Scheme 1. The procedures were similar to that described for compound **4** with O-methylhydroxylamine hydrochloride was used instead of hydroxylamine hydrochloride.

1-((1-Benzyl-1H-1,2,3-triazol-4-yl)methyl)-3-(methoxyimino)indolin-2-one (5a) Yellow solid; Yield: 58%. mp: 209–210 °C. $R_f = 0.59$ (DCM: MeOH = 20: 1). IR (KBr, cm^{-1}): 3063 (CH, arene); 2903 (CH, CH_2); 1717 (C=O); 1607, 1464 (C=C). $^1\text{H-NMR}$ (500 MHz, DMSO- d_6 , ppm): 8.18 (1H, s, H-6'), 7.89 (1H, d, $J = 2.50$ Hz, H-4), 7.44 (1H, d, $J = 7.50$ Hz, H-6), 7.37–7.32 (3H, m, H-4", H-5", H-6"), 7.27 (2H, d, $J = 8.50$ Hz, H-3", H-7"), 7.13 (1H, d, $J = 8.00$ Hz, H-7), 7.10 (1H, t, $J = 7.50$ Hz, H-5), 5.55 (2H, s, H-1"a, H-1"b), 4.98 (2H, s, H-1'a, H-1'b), and 4.22 (3H, s, NOCH_3). ^{13}C NMR (125 MHz, DMSO- d_6 , ppm): δ 162.45, 143.72, 143.69, 142.53, 136.42, 133.33, 129.20, 128.60, 128.36, 127.79, 124.06, 123.38, 115.47, 110.41, 65.01, 53.29, and 35.26. ESI-MS m/z : 348.10 [M + H] $^+$

1-((1-Benzyl-1H-1,2,3-triazol-4-yl)methyl)-5-fluoro-3-(methoxyimino)indolin-2-one (5b) Yellow solid; Yield: 55%. mp: 215–216 °C. $R_f = 0.60$ (DCM: MeOH = 20: 1). IR (KBr, cm^{-1}): 2984 (CH, arene); 2901 (CH, CH_2); 1711 (C=O); 1599, 1476 (C=C). $^1\text{H-NMR}$ (500 MHz, DMSO- d_6 , ppm): 8.18 (1H, s, H-6'), 7.70 (1H, dd, $J = 8.25$ Hz, $J' = 2.50$ Hz, H-4), 7.44–7.31 (4H, m, H-4, H-4", H-5", H-6"), 7.27 (2H, d, $J = 8.00$ Hz, H-3", H-7"), 7.15 (1H, dd, $J = 8.50$ Hz, $J' = 4.00$ Hz, H-6), 5.55 (2H, s, H-1"a, H-1"b), 4.99 (2H, s, H-1'a, H-1'b), and 4.24 (3H, s, NOCH_3). ^{13}C

NMR (125 MHz, DMSO-*d*₆, ppm): δ 162.32, 159.45, 157.55, 143.42, 142.40, 140.09, 136.41, 129.21, 128.61, 128.37, 124.08, 119.67, 119.48, 116.01, 115.93, 114.93, 114.72, 111.55, 111.48, 65.25, 53.30, and 35.39. *ESI-MS* *m/z*: 366.10 [M + H]⁺

1-((1-Benzyl-1H-1,2,3-triazol-4-yl)methyl)-5-chloro-3-(methoxyimino)indolin-2-one (5c) Yellow solid; Yield: 54%. mp: 224–225 °C. *R_f* = 0.63 (DCM: MeOH = 20: 1). *IR* (KBr, cm⁻¹): 2986 (CH, arene); 2901 (CH, CH₂); 1711 (C=O); 1605, 1468 (C=C). ¹H-NMR (500 MHz, DMSO-*d*₆, ppm): 8.18 (1H, s, H-6'), 7.88 (1H, d, *J* = 2.00 Hz, H-4), 7.53 (1H, dd, *J* = 8.50 Hz, *J'* = 2.00 Hz, H-7), 7.37–7.32 (3H, m, H-4'', H-5'', H-6''), 7.27 (2H, d, *J* = 8.00 Hz, H-3'', H-7''), 7.17 (1H, d, *J* = 8.50 Hz, H-6), 5.55 (2H, s, H-1''a, H-1''b), 5.00 (2H, s, H-1'a, H-1'b), and 4.25 (3H, s, NOCH₃). ¹³C NMR (125 MHz, DMSO-*d*₆, ppm): δ 162.12, 142.93, 142.50, 142.31, 136.39, 132.56, 129.21, 128.61, 128.38, 112.21, 127.05, 124.08, 116.64, 112.02, 65.33, 53.31, and 35.42. *ESI-MS* *m/z*: 382.10 [M + H]⁺

1-((1-Benzyl-1H-1,2,3-triazol-4-yl)methyl)-7-chloro-3-(methoxyimino)indolin-2-one (5d) Yellow solid; Yield: 50%. mp: 229–230 °C. *R_f* = 0.63 (DCM: MeOH = 20: 1). *IR* (KBr, cm⁻¹): 2986 (CH, arene); 2903 (CH, CH₂); 1713 (C=O); 1603, 1441 (C=C). ¹H-NMR (500 MHz, DMSO-*d*₆, ppm): 8.15 (1H, s, H-6'), 7.96 (1H, dd, *J* = 7.50 Hz, *J'* = 1.00 Hz, H-4), 7.45 (1H, dd, *J* = 8.25 Hz, *J'* = 1.25 Hz, H-6), 7.37–7.32 (3H, m, H-4'', H-5'', H-6''), 7.25 (2H, d, *J* = 8.00 Hz, H-3'', H-7''), 7.13 (1H, t, *J* = 7.75 Hz, H-5), 5.55 (2H, s, H-1''a, H-1''b), 5.31 (2H, s, H-1'a, H-1'b), and 4.26 (3H, s, NOCH₃). ¹³C NMR (125 MHz, DMSO-*d*₆, ppm): δ 163.35, 144.02, 142.48, 139.57, 136.55, 135.16, 129.18, 128.54, 128.20, 126.85, 124.86, 123.33, 118.51, 115.49, 65.41, 53.26, and 37.72. *ESI-MS* *m/z*: 382.10 [M + H]⁺

1-((1-Benzyl-1H-1,2,3-triazol-4-yl)methyl)-5-bromo-3-(methoxyimino)indolin-2-one (5e) Yellow solid; Yield: 54%. mp: 234–235 °C. *R_f* = 0.65 (DCM: MeOH = 20: 1). *IR* (KBr, cm⁻¹): 2986 (CH, arene); 2901 (CH, CH₂); 1719 (C=O); 1603, 1465 (C=C). ¹H-NMR (500 MHz, DMSO-*d*₆, ppm): 8.18 (1H, s, H-6'), 8.00 (1H, d, *J* = 1.50 Hz, H-4), 7.53 (1H, dd, *J* = 8.50 Hz, *J'* = 2.00 Hz, H-7), 7.37–7.32 (3H, m, H-4'', H-5'', H-6''), 7.27 (2H, d, *J* = 8.00 Hz, H-3'', H-7''), 7.12 (1H, d, *J* = 8.50 Hz, H-6), 5.55 (2H, s, H-1''a, H-1''b), 4.99 (2H, s, H-1'a, H-1'b), and 4.25 (3H, s, NOCH₃). ¹³C NMR (125 MHz, DMSO-*d*₆, ppm): δ 162.01, 142.89, 142.80, 142.30, 136.39, 135.59, 129.72, 129.21, 128.61, 128.37, 124.07, 117.08, 114.84, 112.51, 65.35, 53.31, and 35.40. *ESI-MS* *m/z*: 426.10 (⁷⁹Br), 428.10 (⁸¹Br) [M + H]⁺

1-((1-Benzyl-1H-1,2,3-triazol-4-yl)methyl)-3-(methoxyimino)-5-methylindolin-2-one (5f) Yellow solid; Yield: 62%. mp: 218–219 °C. *R_f* = 0.64 (DCM: MeOH = 20: 1). *IR* (KBr, cm⁻¹): 2986 (CH, arene); 2903 (CH, CH₂); 1713 (C=O); 1614, 1483 (C=C). ¹H-NMR (500 MHz, DMSO-*d*₆, ppm): 8.16 (1H, s, H-6'), 7.73 (1H, s, H-4), 7.37–7.24 (6H, m, H-7, H-3'', H-4'', H-5'', H-6'', H-7''), 7.01 (1H, d, *J* = 8.00 Hz, H-6), 5.55 (2H, s, H-1''a, H-1''b), 4.95 (2H, s, H-1'a, H-1'b), 4.22 (3H, s, NOCH₃), and 2.28 (3H, s, 5-CH₃). ¹³C NMR (125 MHz, DMSO-*d*₆, ppm): δ 162.46, 143.82, 142.62, 141.49, 136.43, 133.52, 132.47, 129.20, 128.60, 128.36, 128.24, 124.03, 115.52, 110.18, 64.96, 53.28, 35.26, and 20.93. *ESI-MS* *m/z*: 362.10 [M + H]⁺

1-((1-Benzyl-1H-1,2,3-triazol-4-yl)methyl)-5-methoxy-3-(methoxyimino)indolin-2-one (5g) Yellow solid; Yield: 50%. mp: 224–225 °C. *R_f* = 0.62 (DCM: MeOH = 20: 1). *IR* (KBr, cm⁻¹): 3007 (CH, arene); 2812 (CH, CH₂); 1719 (C=O); 1597, 1477 (C=C). ¹H-NMR (500 MHz, DMSO-*d*₆, ppm): 8.16 (1H, s, H-6'), 7.88 (1H, s, H-4), 7.36–7.35 (3H, m, H-4'', H-5'', H-6''), 7.27 (2H, d, *J* = 8.00 Hz, H-3'', H-7''), 7.05–7.03 (2H, m, H-6, H-7), 5.55 (2H, s, H-1''a, H-1''b), 4.95 (2H, s, H-1'a, H-1'b), 4.22 (3H, s, NOCH₃), and 3.74 (3H, s, 5-OCH₃). ¹³C NMR (125 MHz, DMSO-*d*₆, ppm): δ 162.31, 155.77, 143.93, 142.60, 137.31, 136.43, 129.21, 128.61, 128.37, 124.02, 118.13, 116.02, 114.15, 111.04, 65.08, 56.50, 56.23, 53.27, and 35.29. *ESI-MS* *m/z*: 378.10 [M + H]⁺

AChE inhibition assay

Evaluation of the AChE inhibition activities was conducted using the previously reported Ellman's method (Ellman et al. 1961) with slight modifications. In brief, to 60 μL of 50 mM NaHPO₄ buffer (pH 7.7) were added 10 μL of respective assayed sample (at stock solution of 0.5 mM). Then, 10 μL of enzyme (0.005 unit enzyme per well) was added. The resulting contents were mixed and pre-read at 405 nm, then the contents were preincubated for 10 min at 37 °C. The reaction in each well was initiated by the addition of 10 μL of 0.5 mM substrate (acetylthiocholine iodide or butyrylthiocholine bromide) to each well, followed by the addition of 10 μL DTNB (0.5 mM per well). The wells were incubated for at 37 °C, then the absorbance of each well was measured at 405 nm using 96-well plate reader Synergy HT, Biotek, USA. All experiments were carried out in triplicate. Eserine (0.5 mM) was used as a positive control. The inhibition percentages were calculated by the following formula:

$$\text{Inhibition Percentage} = \frac{\text{Control}_{\text{Abs}} - \text{Sample}_{\text{Abs}}}{\text{Control}_{\text{Abs}}} \times 100$$

IC₅₀ values (in case measured) were calculated using EZ-Fit Enzyme kinetics software (Perrella Scientific Inc. Amherst, USA).

DPPH radical-scavenging assay

DPPH radical-scavenging activity was measured according to a described method (Thuong et al. 2006). Briefly, 5 µl of each sample dissolved in MeOH were added to 195 µl of 150 µM methanolic DPPH in 96-well plates. The solution was mixed for 1 min and incubated at room temperature in a dark place. After 30 min, the absorbance of the reaction mixture was measured at 520 nm on a microplate reader. The scavenging activity was expressed as the degree of radical reduction of a test group, in comparison with that of the control.

Cytotoxicity assay

Compounds were initially dissolved in dimethyl sulfoxide (DMSO) and diluted to appropriate concentrations by culture medium. The media, sera and other reagents that were used for cell culture in this assay were obtained from GIBCO Co. Ltd. (Grand Island, New York, USA). The cells were culture in Dulbecco's Modified Eagle Medium until confluence. The cells were then trypsinized and suspended at 3×10^4 cells/mL of cell culture medium. On day 0, each well of the 96-well plates was seeded with 180 µL of cell suspension. The plates were then incubated in a 5% CO₂ incubator at 37 °C for 24 h. Then 20 µL of each compounds' samples, which were prepared as described above, were added to each well of the 96-well plates, which had been seeded with cell suspension and incubated for 24 h, at various concentrations. The plates were further incubated for 48 h. Cytotoxicity of the compounds was measured by the SRB colorimetric method, as described previously (Skehan et al. 1990) with slight modifications (Ye et al. 2007; Thuong et al. 2006; Kim et al. 2002; Nam et al. 2004). The IC₅₀ values were calculated using a Probits method (Wu et al. 1992) and were averages of three independent determinations (SD ≤ 10%).

Docking studies

Molecular docking was carried out with the 3D X-ray crystal structure of the target enzyme human AChE downloaded from the Protein Data Bank (PDB ID: 4EY7) (Cheung et al. 2012). The target structure was imported into the Molsoft. icm-pro.v3.8.3 GUI (<http://www.molsoft.com/icmpro/>) (An et al. 2005; Neves et al. 2012); then the co-ligand Donepezil and water molecules were removed from the protein complex. After that the hydrogens and other amino acids such as His, Pro, Gly, Cys were optimized and the missing side chains were also fixed (Arthur and Uzairu 2019). The 3D structures

of synthesized compounds were built using the Builder module of Molecular Operating Environment (MOE) 2019.01 (MOE 2019; Tung et al. 2013; Nam et al. 2014). They were minimized using molecular mechanic force field (MM+) option in order to remove all strain from the molecular structures. Docking assays were performed based on the search algorithm Monte-Carlo implemented into Internal Coordinates Mechanics (ICM) package, keeping the protein rigid and the ligands flexible (Arthur and Uzairu 2019). To quantifying the binding affinity, ICM scoring function was computed based on the parameters: (i) internal force-field energy of the ligand, (ii) entropy loss of the ligand between bound and unbound states, (iii) ligand-receptor hydrogen bond interactions, (iv) polar and nonpolar solvation energy differences between bound and unbound states, (v) electrostatic energy, (vi) hydrophobic energy, and (vii) hydrogen bond donor or acceptor desolvation (Huang and Mucke 2012; Neves et al. 2012). The lower the ICM score (kCal/mol), the higher the chance the ligand is a binder. Biovia DS visualiser was utilized to show up the potential interactions of the ligands to the residues in the binding sites of AChE enzyme (Dassault Systèmes BIOVIA 2016).

Results and discussions

Chemistry

The designed compounds **3a–g** were synthesized by a two-step pathway as illustrated in Scheme 1. A nucleophilic substitution between propargyl bromide and isatins (**1a–g**) was proceeded smoothly in dimethylformamide (DMF) under basic conditions (K₂CO₃). A catalytic amount of KI and gentle heating (60 °C) afforded the intermediates **2a–g** in quantitative yields. In the next step, a Click reaction between the propargyl intermediates **2a–g** and azido-methylbenzene resulted in the target compounds **3a–g** in relatively good yields (55–70%). Condensation of compounds **3a–g** with hydroxylamine.HCl or methoxyamine.HCl in methanol (MeOH) at room temperature gave compounds **4a–g** and **5a–g**, respectively, in moderate yields.

The structures of the synthesized compounds were determined straightforwardly based on analysis of spectroscopic data, including IR, MS, ¹H and ¹³C NMR. In the ¹H-NMR spectra of all compounds, there were always two singlets, each interpreted for 2H, appeared around 5.00 and 5.50 ppm. These singlets were from two methylene groups in the structures. Also in the ¹H-NMR spectra of all compounds, there appeared a singlet at around 8.15–8.18 ppm, interpreted for 1H, which was distinguished for the lone aromatic proton on the triazole ring. All other evidences from IR, MS, ¹H, and ¹³C NMR spectra confirmed the expected structures of compounds **3a–g**, **4a–g**, and **5a–g**.

Bioactivity

AChE inhibitory activity

The synthesized compounds **3a–g**, **4a–g**, and **5a–g** were screened for their inhibitory effects on AChE at two concentrations of 50 and 100 μM . The acetylcholinesterase inhibitor screening kit (colorimetric, BioVision (catalog #K197-100)) was used. The detection was kinetically measured at 412 nm over 40 min. The enzyme inhibition percentages in comparison with donepezil, which was used as a positive control, at the final point were presented in Fig. 3. It was found that at the concentrations of 100 μM , 12 out of 21 compounds showed significant inhibition percentages. Compounds **4g** and **3a** were the most potent in the inhibition of AChE with inhibition percentages of 51% and 50%, respectively. Compounds **3e**, **3f**, and **3g** were among the next most potent with inhibition percentages of 38%, 43%, and 40%, respectively. Compounds **3b** and **3c** were slightly less potent with inhibition percentages of only 31% and 28%, respectively. In overall, the compounds in series **3a–g** appeared to be more potent than those in series **4a–g** and **5a–g**. Introduction of the 3-oxime group on the 2-oxindoline moiety seemed to lower the AChE inhibitory activity. Meanwhile the 3-methoxime functionality on this 2-oxindoline system greatly reduce the bioactivity of the resulting compounds **5a–g**. Exception was observed with compounds **3g**, **4g**, and **5g**, which were substituted with the methoxy group at position 5 on the 2-oxindoline ring. The

order of AChE inhibitory potency was found to be **4g** (51%) > **3g** (40%) > **5g** (26%).

When the assay concentration was lowered to 50 μM , it was found that only compound **4g** showed significant inhibitory activity with an inhibition percentage of 35% in relation to the positive control donepezil. Some other compounds, such as **3a**, **3b**, **3e**, **3f**, **3g**, and **4e** exhibited only minimal inhibition with inhibition percentages of ~11–16%.

The obtained results above suggest that the designed structures **3a–g**, **4a–g**, and **5a–g**, were, though still not strong AChE inhibitors, did exhibit AChE inhibition potentials. Further structural manipulation on the benzyl moiety or substitution patterns at positions 3 or 5 on the 2-oxindoline could potentially produce more novel and potent AChE inhibitors.

DPPH antioxidant activity

Since the antioxidant properties would be an added value to treat AD, the free radical-scavenging abilities of the synthesized compounds against DPPH were screened and the results were summarized in Table 1. The compounds were tested at the initial concentrations of 100 $\mu\text{g}/\text{mL}$. It was found that only two compounds, including **3a** and **3f**, displayed moderate free radical quenching effects in DPPH assay with the inhibition percentages of free radical formation of 38.54 and 37.54%. Several other compounds, including **3d**, **3e**, **3g**, **4a**, **4d**, **4g**, and **5d** showed weak activity. Other compounds exhibited no quenching ability at the assayed concentrations. The results indicate that these structure were not potential as free radical scavengers.

Cytotoxicity against some cancer cell lines

With the available in-house cytotoxic screening system, the synthesized compounds were also screened for their cytotoxicity against three human cancer cell lines, which included SW620 (colorectal adenocarcinoma), PC3 (prostate adenocarcinoma), and NCI-H23 (adenocarcinoma, non-small cell lung cancer) using SRB method. 5-FU (5-fluorouracil), and ADR (adriamycin) were used as positive controls. The results are presented in Table 2. It was very interesting that we found five compounds, including **3c**, **3e**, **5c**, **5e**, and **5g**, with potent cytotoxicity against all three cancer cell lines tested (IC_{50} values in the range of 0.65–7.17 μM). Substitution of the chloro or bromo groups at position 5 seemed to be favorable for cytotoxicity, meanwhile the same chloro substituent at position 7 led to compounds (**3d** and **5d**) with much weaker cytotoxicity (IC_{50} values in the range of 13.56–21.11 μM). The oxime series (**4a–g**) were least cytotoxic among three series; even two compounds **4c** and **4e** also displayed much higher IC_{50}

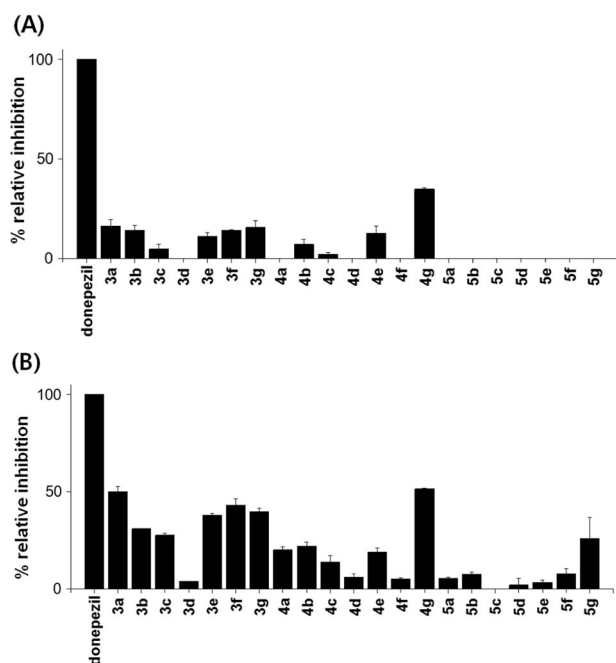
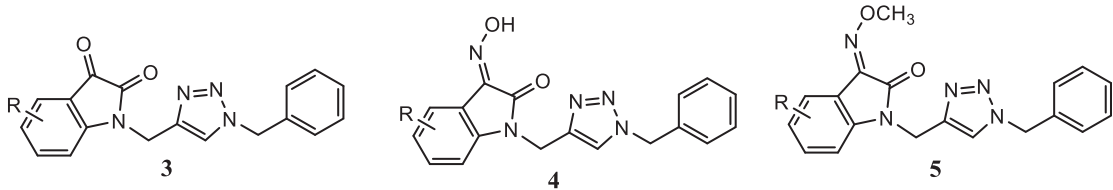


Fig. 3 Relative inhibition of AChE by the compounds synthesized. **a** At concentrations of 50 μM . **b** At concentrations of 100 μM

Table 1 DPPH scavenging activity of the synthesized compounds


Cpd	R	% inhibition ^a	Cpd	R	% inhibition	Cpd	R	% inhibition
3a	H	38.54	4a	H	14.95	5a	H	–
3b	5-F	^b	4b	5-F	4.32	5b	5-F	–
3c	5-Cl	–	4c	5-Cl	4.65	5c	5-Cl	–
3d	7-Cl	7.97	4d	7-Cl	13.29	5d	7-Cl	9.63
3e	5-Br	16.94	4e	5-Br	5.98	5e	5-Br	–
3f	5-CH ₃	37.54	4f	5-CH ₃	–	5f	5-CH ₃	–
3g	5-OCH ₃	16.28	4g	5-OCH ₃	18.27	5g	5-OCH ₃	–
Quercetin		87.71	Quercetin		87.71	Quercetin		87.71

^aInhibition percentages at the concentration of 100 µg/mL

^bNegligible inhibition

values compared with that of compounds **3c**, **3e** and **5c**, **5e**. Strikingly, compound **5g** with 5-methoxy substituent showed the most potent cytotoxicity with IC₅₀ values similar to or even lower than that of adriamycin. Surprisingly, the corresponding compounds in series 3 and 4 (compounds **3g** and **4g**) exhibited only moderate cytotoxicity. Thus, the substituents as well as substituent's positions seemed to play very delicate effects on the cytotoxicity. It was very noteworthy to find a simple structure **5g** with such potent cytotoxicity and this compound would serve as an important lead for further design of more potential anticancer agents.

Analysis of apoptosis of compound **5g**

From the SRB assay **5g** emerged as the most cytotoxic compound three human cancer cell lines, even more potent than ADR (adriamycin). With its interesting cytotoxicity, we decided to perform an Annexin V-FITC/propidium iodide (PI) dual staining assay to see whether compounds **5g** can induce apoptosis. During early apoptosis, phosphatidylserine (PS) locates on the cytosolic (inner) side of the cell membrane, and translocates to the extracellular (outer) surface. Because annexin V has a high affinity for PS, so when it is fluorescently labeled with fluorescein isothiocyanate (FITC), it can be used to identify early-stage apoptotic cells. PI is a fluorescent intercalating agent that cannot cross the membrane of live cells. The membranes of cells in the later stages of apoptosis and dead cells are permeable to

PI, and their nuclei stain red. So, severe and late apoptotic cells are stained with both annexin V and PI. Meanwhile, necrotic cells are stained with PI only. We treated U937 (lymphoma cancer) and SW620 (colon cancer) cells with the compound at 50 µM for 24 h and stained the cells with Annexin V-FITC and PI. PAC-1 (the first procaspase activating compound) was used as a positive control. The results shown in Fig. 4 clearly indicate that in U937 cells, compound **5g** only moderately increased late apoptotic cells but strongly induced necrotic cells. The positive control, PAC-1, meanwhile strongly induced U937 cells into late stage of apoptosis (45.4%). In SW620 cells the effects of compound **5g** was seen differently. Compound **5g** caused necrosis in only 11.22% of cell population. Morphologically, compound **5g** caused SW620 cells flatten in almost a similar manner PAC-1 did (Fig. 5).

Docking studies against AChE

From the synthesized compounds, **3a** and **4g** showed acceptable inhibition activity against AChE enzyme. Therefore we decided to use molecular docking simulations to get more insight into structure–activity relationships of these derivatives through the binding domain of AChE–Donepezil complex (Cheung et al. 2012). Docking protocol was validated by redocking the co-crystallized Donepezil with the enzyme target. Root-mean square deviation (RMSD) was used to evaluate how different the redocked configuration is from the corresponding co-crystal

Table 2 Cytotoxicity of the compounds against some human cancer cell lines

Cpd	R	MW	LogP ^a	Cytotoxicity (IC ₅₀ , ^b μM)/Cell lines ^c		
				SW620	PC3	NCI-H23
3a	H	318.2	1.66	19.54 ± 1.78	>30	>30
3b	5-F	336.1	1.86	13.32 ± 2.11	15.85 ± 2.56	11.54 ± 1.98
3c	5-Cl	352.1	2.31	3.93 ± 0.52	7.17 ± 0.14	5.35 ± 0.07
3d	7-Cl	352.1	2.31	17.43 ± 1.45	14.22 ± 1.31	13.56 ± 1.76
3e	5-Br	398.1	2.55	3.49 ± 0.06	3.68 ± 0.07	4.30 ± 1.11
3f	5-CH ₃	332.1	2.21	25.25 ± 1.87	28.43 ± 2.19	>30
3g	5-OCH ₃	348.1	1.74	27.43 ± 2.09	23.21 ± 2.00	20.14 ± 1.90
4a	H	333.2	3.74	25.46 ± 2.11	>30	>30
4b	5-F	351.1	3.94	13.47 ± 1/56	15.32 ± 1.78	19.32 ± 1.99
4c	5-Cl	367.1	4.39	10.55 ± 1.01	12.21 ± 1.19	11.53 ± 1.13
4d	7-Cl	367.1	4.39	17.21 ± 1.90	19.20 ± 1.89	23.33 ± 2.01
4e	5-Br	413.1	4.63	9.29 ± 0.81	13.21 ± 1.22	15.43 ± 1.31
4f	5-CH ₃	347.1	4.29	21.01 ± 1.90	23.54 ± 1.32	20.12 ± 1.97
4g	5-OCH ₃	363.1	3.82	15.93 ± 1.42	16.23 ± 1.45	18.31 ± 1.75
5a	H	347.1	3.71	>30	25.31 ± 2.16	27.33 ± 2.65
5b	5-F	365.1	3.92	18.31 ± 1.56	20.11 ± 1.95	22.43 ± 2.03
5c	5-Cl	381.1	4.36	2.32 ± 0.55	2.62 ± 0.61	2.87 ± 0.29
5d	7-Cl	381.1	4.36	21.11 ± 2.05	17.21 ± 1.67	15.23 ± 1.35
5e	5-Br	427.1	4.61	1.49 ± 0.02	1.59 ± 0.21	1.40 ± 0.20
5f	5-CH ₃	361.1	4.26	10.31 ± 0.92	9.34 ± 0.74	14.32 ± 1.21
5g	5-OCH ₃	377.1	3.80	0.65 ± 0.03	1.11 ± 0.13	0.99 ± 0.10
5-FU^d		130.08	-0.81	8.84 ± 1.92	13.61 ± 0.46	13.45 ± 3.92
ADR^e		543.5	1.27	1.12 ± 0.14	1.16 ± 0.28	1.29 ± 0.12
PAC-1^f		392.49	3.43	5.82 ± 0.20	4.16 ± 0.52	5.32 ± 0.21

^aCalculated by ChemDraw 9.0 software^bThe concentration (μM) of compounds that produces a 50% reduction in enzyme activity or cell growth, the numbers represent the averaged results from triplicate experiments with deviation of <10%^cCell lines: SW620, colon cancer; PC3, prostate cancer; NCI-H23, lung cancer^d5-FU: 5-Fluorouracil, a positive control^e5-ADR: Adriamycin, a positive control^fPAC-1: The first procaspase-3 activating compound, a positive control

Donepezil. As the results, redocked structure of this drug is highly overlapped with the co-crystal ligand (RMSD = 0.22 Å) and docking score was -25.28 kCal/mol (Fig. 6). In addition, the redocked and co-crystal Donepezil showed similar interactions with the binding site of AChE. The 5,6-dimethoxy-1-indanone moiety of the drug forms multiple interactions with the residues at the peripheral anionic site

(PAS) of AChE, such as π-π interactions with Trp286 and H-bonds with Tyr72, Ser293, and Tyr341. The piperazine ring interacts with acyl-binding pocket through multiple π-π interactions with Tyr337 and Phe338 side chains. Meanwhile the phenyl moiety of Donepezil mainly interact with the choline-binding site and forms strong π-π stacking interactions against Trp86 aromatic side chain. These results

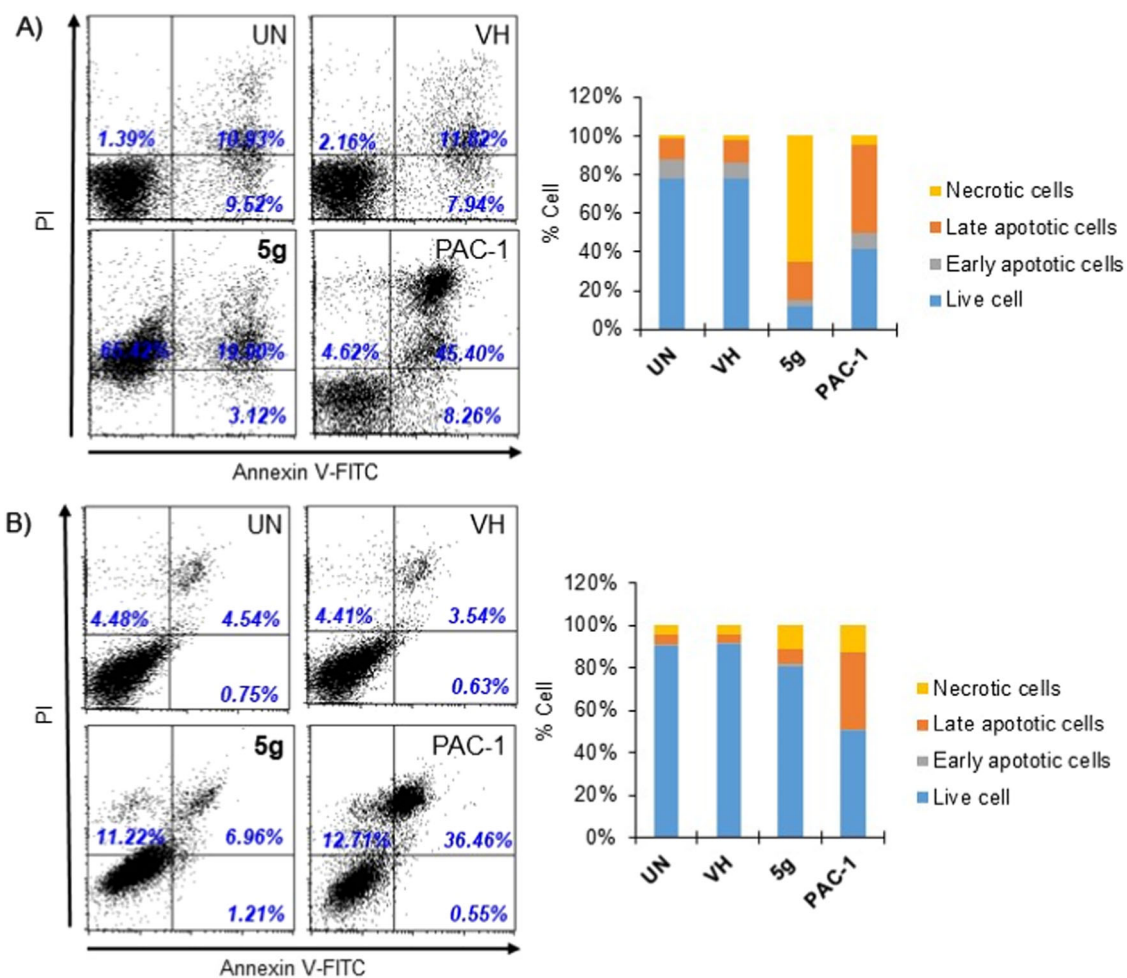
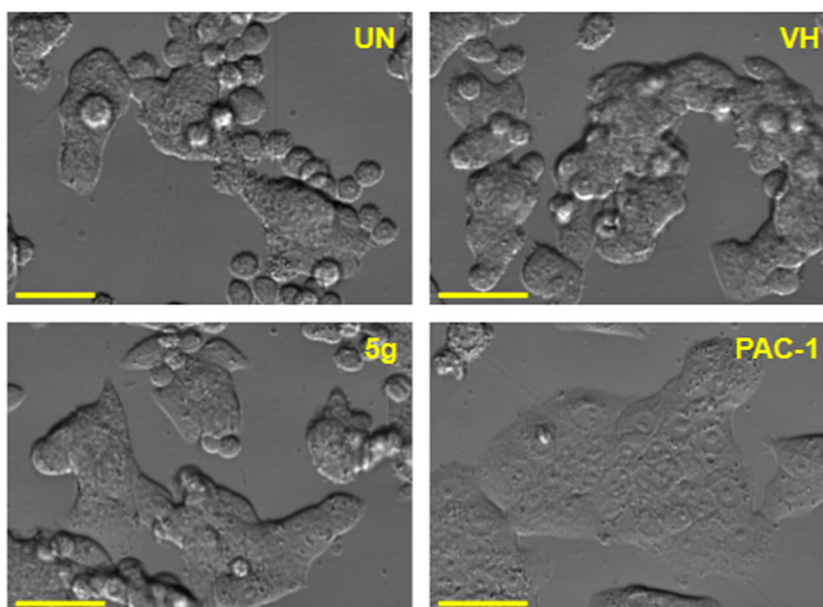


Fig. 4 Apoptosis (Annexin V/PI) analysis of compound **5g**. U937 (a) or SW620 (b) cells were treated with compounds (50 μM) for 24 h. The harvested cells were incubated with Annexin V-FITC and PI. UN

untreated, VH vehicle (DMSO, 0.05%). PAC-1 is a positive control (the first procaspase activating compound). Area 1: PI positive population, Area 2: Annexin V-positive population

Fig. 5 Morphology changes of cells treated with compound **5g** or PAC-1. SW620 2.5×10^5 cells/ml seeding (500 ml in 24 well) were incubated for 24 h, then compound **5g** or PAC-1 (50 μM) were added and incubated further for 24 h. Then, the cells were photographed using an Imaging Device (celldiscoverer7) with $\times 40$ lens. Scale bar: 50 μm. PAC-1, the first procaspase-3 activating compound, was used as a positive control



are consistent with those previously published (Özdemir et al. 2017; Semenov et al. 2015).

Applying the same docking procedures, we found that compounds **3a** and **4g** could engage some characteristic interactions previously determined for Donepezil with AChE enzyme. The binding affinity of **3a** and **4g** was -19.34 and -21.53 kCal/mol, slightly lower than that of

Donepezil. This results match well with the experimental values. From the docked orientations of these derivatives, as shown in Fig. 7, with comparison with the isatin heterocyclic systems in **3a**, the 1-oxindole heterocyclic systems in **4g** showed higher interactions with the residues in the PAS and acyl pocket of AChE. Compound **4g** provided multiple stacking interactions with Trp286 and three H-bonds with Phe295, Arg296, and Tyr341. The triazole ring of our derivatives show extensive hydrophobic interactions against Phe295 and Tyr341, similar to the interactions provided by the piperazine moiety of Donepezil. In addition, strong H-bond and van der Waals interactions were formed between the 1-benzyl-1*H*-1,2,3-triazole moiety towards Tyr124, suggesting the different conformations in the binding site of synthesized derivatives from the Donepezil structure, as shown in Fig. 7.

Conclusions

In conclusion, we have reported three series of indolin-2-one derivatives incorporating 1-((1-benzyl-1*H*-1,2,3-triazole moiety and evaluated their biological activities, including AChE inhibition, DPPH free scavenging effects and cytotoxicity against three human cancer cell lines (SW620, human colon cancer; PC3, prostate cancer; NCI-H23, lung cancer). Two compounds **4g** and **3a** were the most potent in inhibition of AChE with inhibition percentages of 51 and 50% when tested at the concentration of $100\ \mu\text{M}$. Docking studies with the binding domain of

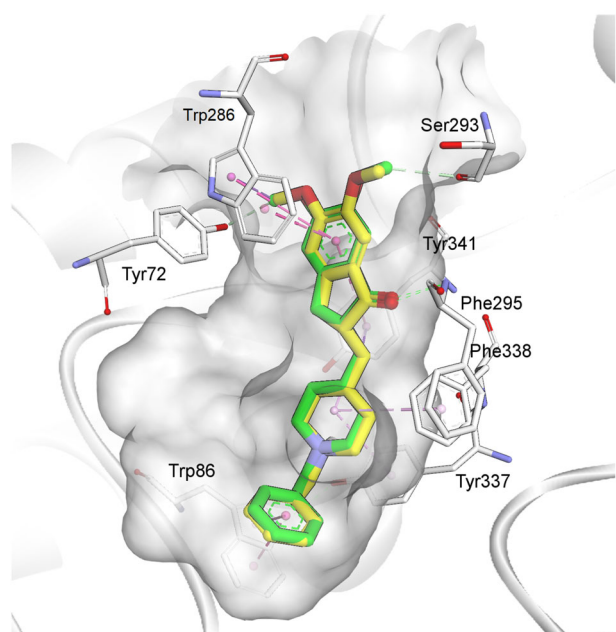


Fig. 6 Superposition of co-crystal (green) and redocked (yellow) Donepezil inside active site of AChE PDB ID 4EY7 structure

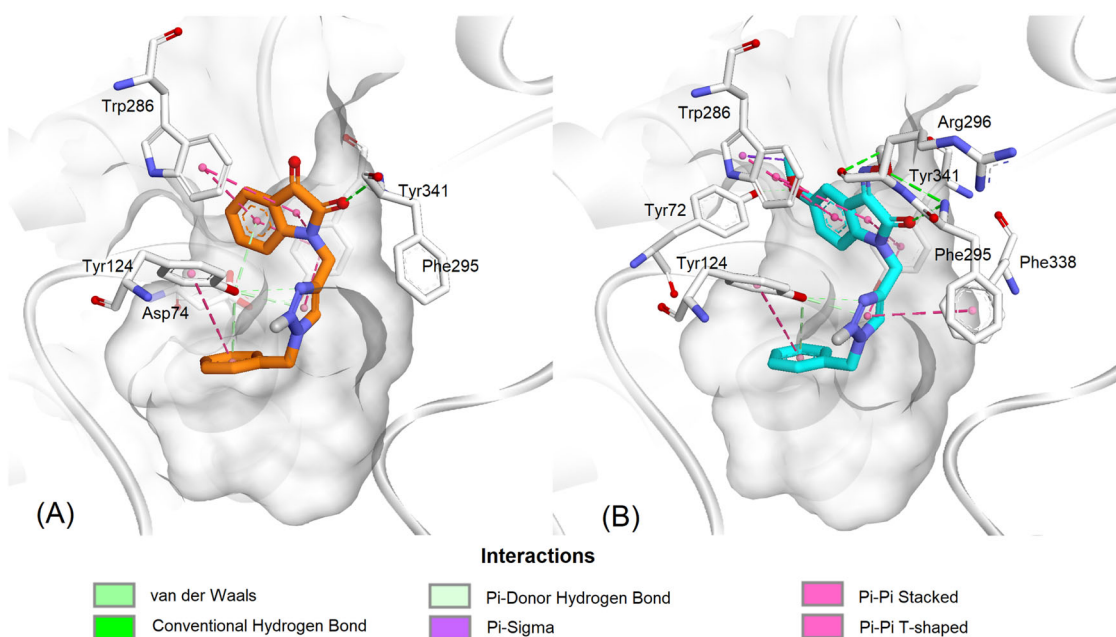


Fig. 7 Docked positions of compound **3a** (a) and **4g** (b) inside active site of AChE PDB ID 4EY7 structure

AChE-Donepezil complex suggested that these compound strictly bound to AChE but with lower affinity compared with the Donepezil molecule. In DPPH free radical-scavenging assay, most compounds showed weak activity. Noteworthy, five compounds, including **3c**, **3e**, **5c**, **5e**, and **5g**, exhibited strong cytotoxicity against three human cancer cell lines. Compound **5g** was the most potent one with IC₅₀ values as low as 0.65 μ M, even more potent than Adriamycin, a positive control. Compound **5g** should be promising for further development as an anticancer agent.

Acknowledgements We acknowledge the principal financial supports from the National Foundation for Science and Technology of Vietnam (NAFOSTED, Grant number 104.01-2018.301). The work was also partly supported by a grant funded by the Korean Government (NRF, Grant number 2017R1A5A2015541).

Compliance with ethical standards

Conflict of interest The authors declare that they have no conflict of interest.

Publisher's note Springer Nature remains neutral with regard to jurisdictional claims in published maps and institutional affiliations.

References

- An J, Totrov M, Abagyan R (2005) Pocketome via comprehensive identification and classification of ligand binding envelopes. *Mol Cell Proteom* 4(6):752
- Arthur DE, Uzairu A (2019) Molecular docking studies on the interaction of NCI anticancer analogues with human phosphatidylinositol 4,5-bisphosphate 3-kinase catalytic subunit. *J King Saud Univ Sci.* 31(4):1151–1166
- Cheung J, Rudolph MJ, Burshteyn F, Cassidy MS, Gary EN, Love J, Franklin MC, Height JJ (2012) Structures of human acetylcholinesterase in complex with pharmacologically important ligands. *J Med Chem* 55(22):10282–10286
- Dassault Systèmes BIOVIA (2016) Discovery studio modeling environment. Accelrys Inc, San Diego, CA, USA
- Ellman GL, Courtney KD, Andres V, Featherstone RM (1961) A new and rapid colorimetric determination of acetylcholinesterase activity. *Bio Pharm* 7(2):88–95
- Huang Y, Mucke L (2012) Alzheimer mechanisms and therapeutic strategies. *Cell* 148(6):1204–1222
- Kim Y, You YJ, Nam NH, Ahn BZ (2002) Prodrugs of 4'-demethyldeoxydopodophyllotoxin: synthesis and evaluation of the anti-tumor activity. *Bioorg Med Chem Lett* 12:3435–3438
- Kumar A, Singh A, Ekavali (2015) A review on Alzheimer's disease pathophysiology and its management: an update. *Pharm Rep.* 67(2):195–203
- Massoulié J, Pezzementi L, Bon S, Krejci E, Vallette F-M (1993) Molecular and cellular biology of cholinesterases. *Prog Neurobiol* 41(1):31–91
- Molecular Operating Environment (MOE) 2019.01 chemical computing group ULC (2019) 1010 Sherbooke St. West, Suite #910, Montreal, QC, Canada, H3A 2R7
- Nam NH, Huong TL, Dung DTM, Dung PTP, Oanh DTK, Park SH, Kim K, Han BW, Yun J, Kang JS, Kim Y, Han SB (2014) Synthesis, bioevaluation and docking study of 5-substitutedphenyl-1,3,4-thiadiazole-based hydroxamic acids as histone deacetylase inhibitors and antitumor agents. *J Enzym Inhib Med Chem* 29(5):611–618
- Nam NH, Pitts RL, Sun S, Sardari S, Tiemo A, Xie M, Yan B, Parang K (2004) Design of tetrapeptide ligands as inhibitors of the Src SH2 domain *Bioorg Med Chem* 12(4):779–787
- Neves MA, Totrov M, Abagyan R (2012) Docking and scoring with ICM: the benchmarking results and strategies for improvement. *J Comput Aided Mol Des* 26(6):675–686
- Olivero G, Grilli M, Chen J, Preda S, Mura E, Govoni S, Marchi M (2014) Effects of soluble β -amyloid on the release of neurotransmitters from rat brain synaptosomes. *Front Aging Neurosci* 6:166
- Özdemir Z, Yılmaz H, Sarı S, Karakurt A, Şenol FS, Uysal M (2017) Design, synthesis, and molecular modeling of new 3(2H)-pyridazinone derivatives as acetylcholinesterase/butyrylcholinesterase inhibitors. *Med Chem Res* 26(10):2293–2308
- Rodda J, Carter J (2012) Cholinesterase inhibitors and memantine for symptomatic treatment of dementia. *BMJ* 344:e2986
- Semenov VE, Zueva IV, Mukhamedyarov MA, Lushchekina SV, Kharlamova AD, Petukhova EO, Mikhailov AS, Podyachev SN, Saifina LF, Petrov KA, Minnekhanova OA, Zobov VV, Nikolsky EE, Masson P, Reznik VS (2015) 6-Methyluracil derivatives as bifunctional acetylcholinesterase inhibitors for the treatment of Alzheimer's disease. *ChemMedChem* 10(11):1863–1874
- Singh M, Kaur M, Kukreja H, Chugh R, Silakari O, Singh D (2013) Acetylcholinesterase inhibitors as Alzheimer therapy: from nerve toxins to neuroprotection. *Eur J Med Chem* 70:165–188
- Skehan P, Storeng R, Scudiero D, Monks A, McMahon J, Vistica D, Warren JT, Bokesch H, Kenney S, Boyd MR (1990) New colorimetric cytotoxicity assay for anticancer-drug screening. *J Natl Cancer Inst* 82(13):1107–1112
- Thuong PT, Na MK, Dang NH, Hung TM, Ky PT, Thanh TV, Nam NH, Thuan ND, Sok DE, Bae KH (2006) Antioxidant activities of Vietnamese medicinal plants. *Nat Prod Sci* 12:29–37
- Tung TT, Oanh DTK, Dung PTP, Hue VT, Park SH, Han BW, Kim Y, Hong JT, Han S-B, Nguyen-Hai N (2013) New benzothiazole/thiazole-containing hydroxamic acids as potent histone deacetylase inhibitors and antitumor agents. *Med Chem* 9(8):1051–1057
- Wu L, Smythe AM, Stinson SF, Mullendore LA, Monks A, Scudiero DA, Paull KD, Koutsoukos AD, Rubinstein LV, Boyd MR, Shoemaker RH (1992) Multidrug-resistant phenotype of disease-oriented panels of human tumor cell lines used for anticancer drug screening. *Cancer Res* 52(11):3029–3034
- Ye G, Nam NH, Kumar A, Saleh A, Shenoy DB, Amiji MM, Lin X, Sun G, Parang K (2007) Synthesis and evaluation of tripodal peptide analogues for cellular delivery of phosphopeptides. *J Med Chem* 50:3604–3617
- Yiannopoulou KG, Papageorgiou SG (2013) Current and future treatments for Alzheimer's disease. *Ther Adv Neurol Disord* 6(1):19–33